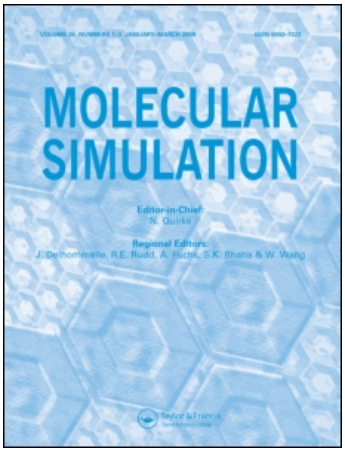

Molecular Simulation
Publication details, including instructions for authors and subscription information:
http://www.informaworld.com/smpp/title~content=t713644482

Topological lattice descriptors of graphene sheets with fullerene-like nanostructures

Franco Cataldo[ab]; Ottorino Ori[ab]; Susana Iglesias-Groth[c]
[a] INAF - Osservatorio Astrofisico di Catania, Catania, Italy [b] Actinium Chemical Research, Rome, Italy
[c] Instituto de Astrofisica de Canarias, La Laguna, Tenerife, Canary Islands, Spain

First published on: 22 January 2010

To cite this Article Cataldo, Franco , Ori, Ottorino and Iglesias-Groth, Susana(2010) 'Topological lattice descriptors of graphene sheets with fullerene-like nanostructures', Molecular Simulation, 36: 5, 341 — 353, First published on: 22 January 2010 (iFirst)
To link to this Article: DOI: 10.1080/08927020903483262
URL: http://dx.doi.org/10.1080/08927020903483262

Molecular Simulation
Vol. 36, No. 5, April 2010, 341–353

Taylor & Francis
Taylor & Francis Group

Topological lattice descriptors of graphene sheets with fullerene-like nanostructures

Franco Cataldo[ab], Ottorino Ori[ab]* and Susana Iglesias-Groth[c]

[a]*INAF – Osservatorio Astrofisico di Catania, Via S. Sofia 78, 95123 Catania, Italy;* [b]*Actinium Chemical Research, Via Casilina, 1626/A 00133 Rome, Italy;* [c]*Instituto de Astrofisica de Canarias, Via Lactea s/n, E-38200 La Laguna, Tenerife, Canary Islands, Spain*

(*Received 29 December 2008; final version received 12 November 2009*)

Polynomial behaviour of the Wiener index for infinite chemical graphs is subject here to a generalisation to structures with topological dimensionality $d_T > 1$. This allows a pure topological analysis of relative chemical stability of graphite lattice portions and fullerene fragments (nanocones) built around a pentagonal face. The Wiener index of the graph acts as a lattice topological potential subject to a minimum principle that is able to discriminate topological structures made of hexagons with different connectivity. A new indicator of graph topological efficiency has been applied in the infinite lattice limit to allow a complete ranking of graph chemical stability. A certain grade of reactivity of the pentagonal ring at the centre of nanocones is also predicted. Our considerations are mainly performed in the dual topological space.

Keywords: topological Wiener index; carbon black; fullerenes; carbon nanostructure

1. Introduction

This paper originates as an attempt to answer the following questions: 'what should a topological analysis tell us about the possibility of formation of fullerene-like structures in carbon black?'. Another interesting question concerns the reactivity of a graphene sheet with a fullerene-like structure: should a topological analysis of a graphene sheet be able to give us an answer about the stability and the reactivity of such carbon nanostructure?

The concept and definition of a fullerene-like structure in a graphene sheet can be found in earlier publications [1,2] and originated from works dealing with the presence of fullerene-like structures [3] and fullerenes [4] in certain carbon blacks and soots. Fullerenic structures also play a role in the soot-formation mechanism [5], and fullerene-like structures are also formed in ball-milled graphite or other carbon materials [6] and even in irradiated graphite where dislocations and displacements of carbon atoms [7] must necessarily generate fullerene-like structures as well [8]. The presence of fullerene-like structures on carbon black graphene sheets or on activated carbon has many important implications, for instance, on the physisorption but especially on the chemisorption sites of macromolecules in rubber- or plastic-based composites reinforced with carbon black or for the adsorption of molecules on the surface of activated carbon, as outlined in a review paper [9]. The importance of fullerene-like structures is not limited only to composites or environmental chemistry, it involves also the interstellar carbon dust. It has been estimated that at least 3% of the mass of our galaxy is locked under the form of carbon dust. This carbon dust rather than being under the form of graphite should instead be under the form of radiation-damaged graphite or under the form of amorphous carbon, i.e. carbon black. Under these forms the interstellar carbon dust should be rich in fullerene-like structures, and therefore should play a crucial role in the formation of molecular hydrogen from atomic hydrogen [10–12] and also in other low-temperature chemical processes. From these considerations, our interest in starting a topological investigation on the stability and reactivity of fullerene-like structures was derived.

In this paper, we show how a pure topological approach is able to individuate suitable lattice descriptors to rank the relative stability of graphenic structures having a common basic element: the presence of hexagonal rings connected in distinct topological ways.

In particular, we study graphenic structures as both graphite lattice portions and fullerene fragments built around a pentagonal face. Our analysis aims to extract the maximum of physico-chemical information from the *Wiener index* $W(N)$, the oldest and most popular topological descriptor, that is defined in [13] as the semi-sum of the minimum distances between all pairs of vertices in a connected chemical graph made by N atoms (see Section 2). As the yearly production of scientific papers on chemical topology subjects is very large, we would like here to point out just some references to understand how our work has been oriented. The number W did move its first step as topological molecular descriptor for alkanes and some of their physico-chemical properties. After more than 60 years, passing through

*Corresponding author. Email: ottorino.ori@alice.it

ISSN 0892-7022 print/ISSN 1029-0435 online

DOI: 10.1080/08927020903483262
http://www.informaworld.com

relevant generalisations made by Hosoya [14] and many other authors, this index still attracts theoreticians on possible new extensions [15–17] and applications [18]. We show some peculiar properties of $W(N)$ when it gets applied to predict the existence of reactive sites in large, hexagon-made, carbon structures.

Remarkably, W behaves as a polynomial of the number of atoms N. This fundamental property was discovered by Bonchev and Mekenyan in their seminal work [19] devoted to the graph-theory explanation of the energy gap in conjugated polymers. This result allows researchers to approach large chemical structures, keeping under control the infinite growth of W just searching for structure-specific polynomial laws. In the following, we see that this operation is moreover quite easy, being basically a mathematical interpolation with polynomials. In this work, we study large fragments of both graphite lattices and fullerene molecules, introducing new specific W polynomials that will enable extensive topological discussions of various chemical implications.

It is worthwhile to notice here that Bonchev and Mekenyan [19] studied several polymers that may be seen as particular cases of graphite fragments; on the other hand, articles [20,21] show that the Wiener index has been used to derive implications about fullerene isomers' stability based on pure topological considerations; in these papers, the Wiener-index values for certain large isomers of fullerene C_{60}, C_{70}, C_{76}, C_{78} have been computed. Article [22] provides Balasubramanian's extended Wiener analysis on fullerenes in the range C_{20}–C_{90}, whereas the extended treaty [23] deals with properties of the Wiener index for systems made with hexagons. This paper may be seen as a continuation of those graph-theoretical studies; in Section 2, we, in fact, give an overview of the Wiener-index definition and how this graph-invariant quantity is related to the concepts of topologically independent vertices and topological molecular stability. Also, we present the original theoretical results from our topological analysis of graphite and fullerene fragments; these results have interesting chemical implications and topological properties of curved fullerene fragments that may play a relevant role in the reactivity of carbon surfaces in different environments as outlined in the beginning of this section.

2. Topological theoretical model

We base our chemical considerations on the Wiener index W of various structures made by assembling a large number of hexagonal rings. This graph descriptor is defined as the semi-sum of the minimum distances between all pairs of vertices V_i and V_j belonging to a given chemical graph G with N nodes. For example, the molecular graph G corresponding to a benzene ring is the hexagon as shown in Figure 1. G is the hydrogen-depleted

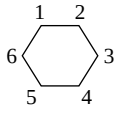

$$D(G) = \begin{matrix} 0 & 1 & 2 & 3 & 2 & 1 \\ 1 & 0 & 1 & 2 & 3 & 2 \\ 2 & 1 & 0 & 1 & 2 & 3 \\ 3 & 2 & 1 & 0 & 1 & 2 \\ 2 & 3 & 2 & 1 & 0 & 1 \\ 1 & 2 & 3 & 2 & 1 & 0 \end{matrix} \qquad W = 27$$

Figure 1. Benzene chemical graph G and its distance matrix; all rows are equivalent; this graph has Wiener index $W = 27$.

chemical graph and N is the number of carbon atoms only: N is either finite (in the case of molecules) or infinite (for polymers or other lattices). The minimum distance d_{ij} equals the number of edges in the shortest path connecting the graph vertex V_i to V_j. For a chemical graph G with N vertices (atoms), we define the graph-invariant Wiener index as

$$W(N) = \frac{1}{2}\sum_{ij} d_{ij}, \quad \text{with } i,j = 1,N; \;\; d_{ii} = 0. \tag{2.1}$$

The distance matrix **D** of the graph G is the symmetric $N \times N$ matrix made with the d_{ij} entries. For the benzene ring ($N = 6$, $W = 27$), **D** is given in Figure 1. Among many ways to write W, we select the following to point out individual contribution w_i (which we also call Wiener weight or WW) coming from each site V_i:

$$W(N) = \frac{1}{2}\sum_{i} w_i, \quad \text{with } i,j = 1,N; \;\; w_i = \sum_{ij} d_{ij}. \tag{2.2}$$

Denoting by M the maximum distance present in the graph $M = \max\{d_{ij}\}$ (i.e. the graph G has a least pair of atoms connected by the shortest path of length M), we arrive at the meaningful formula

$$W(N) = \frac{1}{2}\sum_{im} m b_{im}, \quad \text{with } i = 1,N; \;\; m = 1,M, \tag{2.3a}$$

where b_{im} is the number of m-neighbours of vertex V_i. We call [20,21] the string $\{b_{im}\}$ the Wiener-spectrum (WS) string of vertex V_i. In the case of molecular graphs made of equivalent atoms (e.g. the benzene ring or the $C_{60}(I_h)$ fullerene), WW have the same value, say $\underline{w}$, and Equation (2.3a) then becomes

$$W(N) = \frac{1}{2} N \underline{w}. \tag{2.3b}$$

WS elements b_{im} are subject to the obvious constraints

$$1 + \sum_{m} b_{im} = N, \quad \text{with } i = 1,N. \tag{2.4}$$

By comparing Equations (2.2), (2.3a) and (2.3b), we derive the following relationships for WW:

$$w_i = \sum_m m b_{im}, \quad \text{with } m = 1, M, \tag{2.5a}$$

$$\{b_{im}\} = \{b_{i1} b_{i2} \cdots b_{im} \cdots b_{iM-1} b_{iM}\}, \quad \text{with } m = 1, M, \tag{2.5b}$$

$$\underline{w} = \min\{w_i\}. \tag{2.5c}$$

Any graph has at least one site with minimum w_i value. We write (see Equation (2.5c)) that minimum value as $\underline{w}$ and we call the corresponding vertex V_i the *minimal vertex* of the graph $\underline{V}$. For the benzene graph in Figure 1, all sites play the role of the *minimal vertex* having the same $\underline{w} = 9$ (all rows and columns of **D** in fact produce that sum).

The Wiener index W, WW (w_i) and WS strings $\{b_{im}\}$ are powerful graph descriptors. For example, WS allow us to distinguish in a very direct way topologically inequivalent atoms just taking into account the fact that inequivalent vertices have, in most of the cases, at least one different entry in their $\{b_{im}\}$ sets. Let us study the simple, highly symmetric benzene ring shown in Figure 1; it has the maximum distance $M = 3$ and all six vertices share the same WS set $\{b_{im}\} = \{2\ 2\ 1\}$ since each atom in the ring has two nodes at distance 1, two at distance 2 and one at distance 3. The number of unitary entries in **D** is twice the number of bonds L of the molecule (in this case, thus $L = 6$). By summing each row or column of **D**, we get w_i quantities defined in Equation (2.5a), with $w_i = \underline{w} = 9$; finally, Equation (2.2) produces $W = 27$. Topological markers W, M, L, w_i, $\underline{w}$ are graph invariants.

When we elide a bond in the benzene ring, we obtain a new open graph with diminished symmetry (see Figure 2). This graph, with $M = 5$, has WS string $\{b_{im}\} = \{1\ 1\ 1\ 1\ 1\}$ for symmetric vertices $i = 1,2$; $\{b_{im}\} = \{2\ 1\ 1\ 1\ 0\}$ for $i = 3,6$; $\{b_{im}\} = \{2\ 2\ 1\ 0\ 0\ \}$ for $i = 4,5$. Consequentially, single WW contributions to W are: $w_i = 15$, for $i = 1,2$; $w_i = 11$, for $i = 3,6$; $w_i = 9$, for $i = 4,5$. Vertices V_4 and V_5 are the minimal vertices of G, with $\underline{w} = 9$. We note that this less-symmetric and less-compact open graph has an increased Wiener index $W = 35$ compared to the $W = 27$ value of the benzene ring (Figures 1 and 2).

In this paper, we extensively use the concept of topological compactness of a given graph G with N vertices (carbon atoms), our basal assumption being a topological minimum principle: chemically stable molecular structures tend to minimise their Wiener index. For a molecular structure with N atoms, the Wiener index $W(N)$ given by Equations (2.3a) and (2.3b) assumes its minimum values in correspondence with the most compact isomer that shows shorter distances d_{ij}. According to this pure topological approach, we state that the *most compact isomers will generally show higher chemical stability*. This model produces non-trivial topological and chemical implications only when one compares chemical structures made with similar building units. A heuristic explanation of our approach is found in the physical behaviour of a set of points interconnected by springs; this system made of harmonic oscillators stabilises, at a given fixed temperature, in correspondence with minimum in the sum of the squares of the distances, providing structural compactness to any physically relevant system configurations. Practically, W behaves as the potential energy of a topological long-range interaction, and we use it straight away as *the topological potential energy of the chemical graph G*. From Equation (2.2), we simply compute $W(N)$ by summing WW (w_i) coming from all vertices of G.

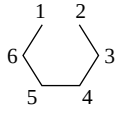

$$D(G) = \begin{matrix} 0 & 5 & 4 & 3 & 2 & 1 \\ 5 & 0 & 1 & 2 & 3 & 4 \\ 4 & 1 & 0 & 1 & 2 & 3 \\ 3 & 2 & 1 & 0 & 1 & 2 \\ 2 & 3 & 2 & 1 & 0 & 1 \\ 1 & 4 & 3 & 2 & 1 & 0 \end{matrix} \qquad W = 35$$

Figure 2. Five-atom chain and its distance matrix; pairs of vertices 1-2, 3-6, 5-4 are equivalent; this graph has Wiener index $W = 35$.

Previous topological studies on fullerenes point out that W is actually able to rank the molecular stability of structures formed by similar subunits and with a similar numbers of vertices N. We just remember here the relevant case of the C_{60} fullerene with its 1812 inequivalent isomers; for this large set of isomers, $W(N)$ reaches its minimum value $W = 8340$ for the physically stable icosahedral 'buckyball' $C_{60}(I_h)$ [24,25] which is therefore also the most topologically compact C_{60} isomer. Moreover, our topological minimum principle on $W(N)$ implies that minimal vertices of G are likely to be the most stable sites of the structure. The molecule will in fact try to preserve the coordination shells around these vertices in order to maintain low w_i contributions to the overall Wiener index according to Equation (2.2).

The present work extends the application of this topological minimum principle on $W(N)$ to various graphenic structures made of a similar number of hexagons (we will study graphitic and fullerenic fragments); these structures will also be analysed in the infinite limit. The possibility of describing the behaviour of $W(N)$ for infinite structures is the most prominent feature of the Wiener index, and it has been discovered by Bonchev and Mekenyan [19] for monodimensional infinite graphs: for a polymer with N atoms, W goes simply as a third-grade polynomial of N.

The general $W(N)$ behaviour is now generalised by the following original conjecture valid in any dimension d_T. For a d_T-dimensional infinite transitionally invariant lattice generated by a unit cell with n_0 atoms, the relative Wiener index is determined by a lattice-specific polynomial, thus $W(Y) \approx Y^{\underline{s}}$, where $\underline{s} = (2d_T + 1)$ and Y represents the

number of unit cells along each edge, e.g. the lattice is made of Y^{d_T} cells and $N = n_0 Y^{d_T}$ vertices. This last relationship implies that the leading power $\underline{k}$ of N in the polynomials for $W(N^{\underline{k}})$ depends on the topological dimensionality d_T of the structure as

$$W(N) = a_{\underline{k}} N^{\underline{k}} + a_{\underline{k}-1} N^{\underline{k}-1} + \cdots + a_1 N + a_0,$$
$$\text{with } \underline{k} = (2d_T + 1)/d_T. \tag{2.6}$$

The new conjecture given by Equation (2.6) is applicable to any infinite periodic graph G, e.g. a graph generated by translating a unit cell. According to Equation (2.6), $W(N)$ polynomials grow as $N^{5/2}$ for two-dimensional graphs and as $N^{7/3}$ for three-dimensional ones; article [26] gave the first indication about the existence of these polynomial laws for the special case of d_T-dimensional tori. For polymers, topological dimensionality $d_T = 1$ gives $\underline{s} = \underline{k} = 3$, and Equation (2.6) reproduces Bonchev and Mekenyan [19] cubic formula for $W(N)$,

$$W(N) = a_3 N^3 + a_2 N^2 + a_1 N + a_0,$$
$$\underline{k} = 3 \text{ for } d_T = 1 \text{ lattices}. \tag{2.7}$$

All coefficients a_j in Equation (2.6) are rational numbers, easily computable by interpolation. Examples of cubic Wiener-index polynomials (2.7) are reported in [19] for several $d_T = 1$ lattices; let us just consider the linear and the zigzag hexagonal polymers represented in Figure 3: we let them symmetrically growing around the unit cell (in this paper, all lattices are formed by an odd number of unit cells) and their Wiener-index polynomials are

$$W(N)_{\text{LIN}} = \frac{(N^3 - N)}{6}, \tag{2.8a}$$

$$W(N)_{\text{ZZ}} = \frac{N^3 + 50N - 144}{12}. \tag{2.8b}$$

In Equation (2.8b), the coefficient $a_0 = -144$ is due to the peculiar unit cell (the eight black atoms represented in Figure 3(b)) selected to generate the periodic lattice; a_0 varies by changing the unit cell shape. We report here the

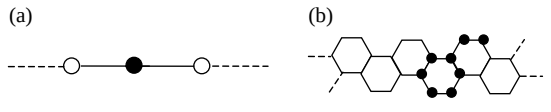

Figure 3. Examples of periodic infinite chemical graphs in one dimension: (a) linear polymer and (b) zigzag hexagonal polymer also classifiable as the graphitic fragment ZZ_1.

original results for the Wiener index W^C computed on the closed $d_T = 1$ lattices (i.e. lattices with periodic boundary conditions):

$$W(N)^C_{\text{LIN}} = \frac{N^3 - N}{8}, \tag{2.9a}$$

$$W(N)^C_{\text{ZZ}} = \frac{N^3 + 64N}{16}. \tag{2.9b}$$

We note here that Equation (2.9a) refers to $d_T = 1$ torus made with an odd number of points, and it is slightly different, in the linear factor, from the formula given earlier in [26] for even-membered tori.

For closed graphs, the dependence of $W(N)$ on a_0 vanishes (as it is natural to expect for a lattice with periodic boundary conditions), and we found on all graphs we tested so far a general numerical behaviour for the ratio W^C/W,

$$\frac{W^C}{W} \to \frac{3}{4},$$
$$\text{when } N \to \infty \text{ for any } d_T = 1 \text{ periodic lattice}. \tag{2.10}$$

The above compression 0.75 ratio is valid for all $d_T = 1$ dimensional lattices that we have studied so far; this fact points out that lattices with periodic boundary conditions are 25% more compact than the corresponding open ones; moreover, we conjecture that the compression factor of Equation (2.10) depends only on lattice topological dimensionality d_T being insensible to the fine structure of the lattice itself. Starting from Equation (2.6), we end this section by introducing a new concept of dimensionality that we call *topological dimensionality* d_T applicable to any structure described by a graph G,

$$d_T = \frac{1}{\underline{k} - 2}. \tag{2.11}$$

This new definition of dimensionality d_T discriminates different topological structures on the basis of the average compactness of their infinite graph. Topological computations indicate so far that d_T assumes *integer* values $d_T = 1,2,3,\ldots$ for infinite *periodic* structures; this paper shows that $d_T = 2$ is valid for non-periodic, infinite nanocone graphs (Figure 7; see Equation (4.4a)).

The following sections are devoted to the analysis of graphitic and fullerenic lattices, and we show how our topological lattice descriptors, Wiener index W (Equation (2.2)), WW (Equation (2.5a)) and WS string (Equation (2.5b)), provide interesting indications on chemical stability and reactivity. All topological formulas are original.

3. Topological analysis of reference graphitic lattice

We start our study from the infinite portions of the graphite lattices generated by a zigzag hexagon ribbon with a thickness of five hexagons (see Figure 4); we call this hexagonal graphitic lattice ZZ_5. Its unit cell is made of 10 hexagonal rings (Figure 4(a)) or, equivalently, of 24 carbon atoms (Figure 4(b)). In the direct space, its unit cell contains 10 hexagons labelled from 1 to 10 (see the arrows in Figure 4(a)). The lattice ZZ_5 is then built by attaching other cells on both sides. Figure 4(a) represents the first step of ZZ_5 lattice growth when just one cell is added in both ways. If ℓ is the *lattice generator* (e.g. the total number of cells in the lattice), then we have that the number N of vertices is $N = 24\ell$. Both graphs in Figure 4 correspond to the ZZ_5 lattice with $\ell = 3$ (in our approach, we prefer to deal with symmetric lattices, thus we consider only odd values of ℓ). We note that the unit cell made of the 24 independent vertices depicted in Figure 4(b) resembles the eight-vertex structure in Figure 3(b) which in fact is the simplest case of zigzag hexagon ribbons, the ZZ_1 lattice. For the ZZ_5 graphitic lattice, we report the results of our topological computations for growing values of ℓ and N.

Case ($\ell = 1$, $N = 24$). The graph corresponds just to the unit cell with 24 atoms in Figure 4. By ordering the graph vertices according to their WW values, we see (Table 1) that all vertices are inequivalent, their WS strings $\{b_{im}\}$ being all different, with the sole temporarily WS degeneracy of V_6/V_{20} and V_1/V_{23} that will vanish for larger values of N. This accidental correspondence $\{b_{6m}\} = \{b_{20m}\}$ does not reflect any structural lattice features since V_6 and V_{20} represent two symmetry-distinct lattice nodes; similar considerations apply to the pair V_1 and V_{23}. These kinds of degeneracy in WS values are solved by increasing the lattice size; the case $\ell = 7$, $N = 168$ already shows, in fact, the independence of these four nodes V_6, V_{20}, V_1, V_{23} and, more in general, of all 24 vertices V_i of the ZZ_5 unit cell (Table 3). If we consider the WW column in Table 1, the first seven starred vertices have minimum w_i values and so, according to our topological model, they are the most strongly bounded to the structure. Our table gives the WW already divided by the factor 2 of Equation (2.2), in such a way that the graph Wiener index $W = 1320$ is easily computed by summing them. We also note that the topological descriptor WS is also able to discriminate the independent sites with the same WW as V_{12} and V_{14}. For this graphitic fragment, we have $W = 1320$, $M = 13$, $L = 28$. This calculation on the 24-atom unit cell shows that the most stable six atoms belong to the central ring $\mathcal{H}$; V_{18} is another stable site of the structure and, in this case, it has also the same WW of V_{18}, but also this accidental degeneracy in WW will disappear for larger values of N (see Table 3).

Case ($\ell = 3$, $N = 72$). We just added a pair of cells to the previous lattice having $\ell = 1$. The most stable sites of this graph (e.g. sites with the lowest values of WW) still belong to the central hexagon $\mathcal{H}$ (Tables 1 and 3), and it gives the lowest WW contributions $w_{\mathcal{H}} = 7974$ to the overall Wiener index $W = 16,544$ when compared to the remaining hexagonal faces. The ring $\mathcal{H}$ is compactly embedded in the graph and V_{13} remains the minimal vertex with the lowest WW value $w_{13} = 340$ and WS sequence $\{b_{13m}\} = \{3\ 6\ 9\ 12\ 15\ 13\ 8\ 4\ 1\}$, where $m = 1, 9$ for V_{13}. This graph has $M = 17$, $L = 96$. On the other hand, among the less stable (most reactive) vertices, we find peripheral atoms as V_{24} with $w_{24}/2 = 270$ and string $\{b_{24m}\} = \{2\ 3\ 5\ 6\ 6\ 6\ 7\ 7\ 6\ 6\ 6\ 5\ 3\ 2\ 1\}$, where $m = 1, 15$ for V_{24}. This result is quite logical, boundary atoms of a graphitic structure being relatively instable.

By increasing N, we obtain, by interpolation, the complete topological characterisation of the graphitic lattice ZZ_5. Table 2 gives the exact original formulas for all topological lattice descriptors Wiener index $W(N)$, number of chemical bonds $L(N)$, maximum graph distance $M(N)$ and their asymptotic limits. Our calculations confirm for

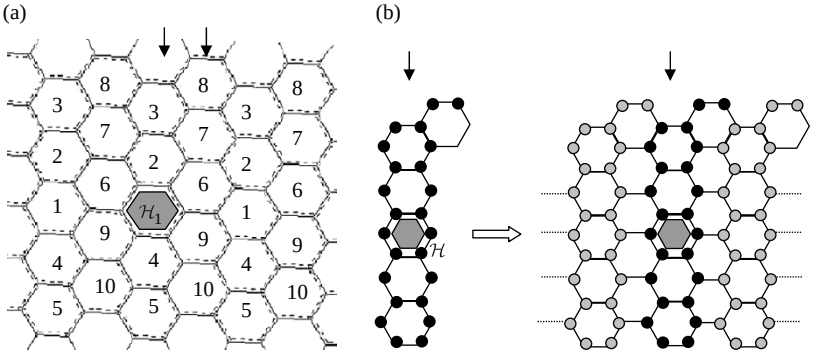

Figure 4. Equivalent representations of the unit cell of the ZZ_5 graphitic linear lattice in the direct space: the arrowed unit cell includes (a) 10 hexagons or (b) 24 bulleted carbon atoms. Both cases represent the three-cell ZZ_5 graph (lattice generator $\ell = 3$); unit cell translations on both sides $\ell = 1,3,5,\ldots$ generate the infinite periodic lattice; the shaded central hexagon $\mathcal{H}$ is the topologically most stable region of the lattice.

Table 1. Graphitic lattice ZZ_5: topological descriptors for 24 vertices V of the unit cell in the $\ell = 1$, $N = 24$ case; only non-zero $\{b_{im}\}$ entries are reported.

V	$\{b_{im}\}$	$w_i/2$	Unit cell view
$^*V_{13}$	3 4 4 4 4 3 1	^{*42}	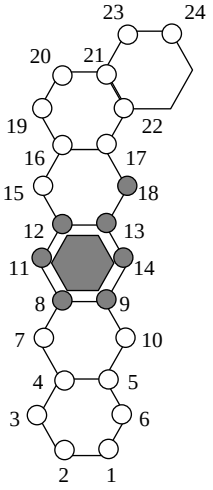
$^*V_{12}$	3 4 4 4 3 3 2	^{*43}	
$^*V_{14}$	2 4 5 4 4 3 1	^{*43}	
$^*V_9$	3 4 4 4 3 2 2 1	^{*44}	
$^*V_{11}$	2 4 5 4 4 2 1 1	^{*44}	
$^*V_8$	3 4 4 4 3 2 1 1 1	^{*45}	
$^*V_{18}$	2 4 5 4 3 2 2 1	^{*45}	
V_{15}	2 4 5 3 3 3 2 1	46	
V_{17}	3 4 4 3 2 2 2 2 1	48	
V_{10}	2 4 5 3 2 2 2 2 1	49	
V_{16}	3 4 3 3 3 2 2 2 1	49	
V_7	2 4 5 3 2 2 2 1 1 1	50	
V_5	3 4 3 2 2 2 2 2 2 1	54	
V_4	3 4 3 2 2 2 2 2 1 1 1	55	
V_{22}	2 4 4 2 2 2 2 2 2 1	55	
V_{19}	2 3 4 3 2 2 2 2 2 1	56	
V_{21}	3 3 2 2 2 2 2 2 2 2 1	62	
V_6	2 3 3 2 2 2 2 2 2 2 1	63	
V_{20}	2 3 3 2 2 2 2 2 2 2 1	63	
V_3	2 3 3 2 2 2 2 2 2 1 1 1	64	
V_1	2 2 2 2 2 2 2 2 2 2 2 1	72	
V_{23}	2 2 2 2 2 2 2 2 2 2 2 1	72	
V_2	2 2 2 2 2 2 2 2 2 2 1 1 1	73	
V_{24}	1 1 2 2 2 2 2 2 2 2 2 2 1	83	

Notes: Most stable graph vertices V have lower WW (w_i) entries and are represented with shaded circles in the unit cell view and belong to the shaded central hexagon $\mathcal{H}$, the most stable ring in the lattice. By summing the last column, one gets the whole Wiener index $W = 1320$ of this graph made of just 24 nodes.

ZZ_5 the polynomial law found by Bonchev and Mekenyan [19] for one-dimensional lattices: $W(N)$ varies, in fact, as a third-grade polynomial of N and, in the limit of large N, it depends only on the cubic power of N. We also defined the polynomial behaviours for M and L. The regularisation threshold of $W(N)$ polynomial occurs at $\ell \geq 5$ ($N \geq 120$), whereas $M(N) = N/6$ stabilises at $\ell \geq 7$ ($N \geq 168$) – we still remember here that only odd ℓ integers are considered by our model to expand the lattices in a symmetric way around the initial unit cell. Table 3 confirms the topological stability of the ring $\mathcal{H}$ also in the case $\ell = 7$.

Let us introduce a newly discovered important polynomial law. Since the Wiener index $W(N)$ coming from a graph with N nodes goes as N^3 (Table 2), we then state the following law: in a monodimensional infinite graph, the contribution to W coming from a single vertex or from a group of them (e.g. a hexagon) varies as a square polynomial of N. In particular, this rule is valid for any polynomial representation of $\underline{w}$ given by Equation (3.1). Our calculations confirm this quadratic behaviour for $w_{\mathcal{H}}$, e.g. the contribution to $W(N)$ coming from the six graph vertices V_j with $j = 8, 9, 11, 12, 13, 14$ of the central hexagon $\mathcal{H}$ (Figure 4 and Table 1). Also, these new polynomial laws, valid in the direct space ZZ_5, stabilise for $\ell \geq 7$ ($N \geq 168$),

$$\underline{w} = w_{13} = \frac{N^2}{24} + 140, \quad \text{for the direct graph } ZZ_5, \quad (3.1)$$

$$w_{\mathcal{H}} = (w_8 + w_9 + w_{11} + w_{12} + w_{14} + w_{13}) = \frac{N^2}{4} + 918, \quad \text{for the direct graph } ZZ_5, \quad (3.2a)$$

$$w_{\mathcal{H}} \to \frac{N^2}{4}, \quad \text{when } N \longrightarrow \infty, \quad \text{for the direct graph } ZZ_5. \quad (3.2b)$$

We remember that the above quantities are divided by 2 when they contribute to $W(N)$ in Equation (2.2). When we compute the same lattice descriptors for the less stable sites of the ZZ_5 graph, we found similar rules; for example, vertex V_{24} has $w_{24} = N^2/24 + 532$ for $\ell \geq 11$ ($N \geq 264$). Thinking of Equation (3.2a), we may similarly calculate the contributions to $W(N)$ related to other hexagonal faces of ZZ_5, reaching the conclusion that all faces contribute to $W(N)$ with quadratic polynomials in N but with values larger than $w_{\mathcal{H}}$.

The central hexagon $\mathcal{H}$ is particularly stable; it corresponds to a region that the lattice tends to preserve its local topology. The barrier to any modification of $\mathcal{H}$ is just provided by the action of $W(N)$ that behaves as the global topological potential energy of the graph. The lattice tends to minimise $W(N)$ values and any bond opening involving $\mathcal{H}$ sites (a bond elision generally causes an increase in Wiener index) is therefore forbidden. We may recognise this topological mechanism in the previous case of the benzene ring where, by cutting one bond, we see a sudden jump in W from $W = 27$ to $W = 35$, about a 30% increase in the topological energy (see Figures 1 and 2). The

Table 2. Topological descriptors for the graphitic monodimensional lattices ZZ_5 (Figure 4) and ZZ_5^D (Figure 5): exact formulas for the Wiener index $W(N)$, the number of chemical bonds $L(N)$, the maximum graph distance $M(N)$ and their values in the infinite N limit are given in direct and dual space.

Descriptor	Direct space ZZ_5	$N \to \infty$	Dual space ZZ_5^D	$N \to \infty$
$W(N)$	$(3N^3+15{,}102N-432{,}432)/108$	$N^3/36$	$N^3/30+115N/6-188$	$N^3/30$
$L(N)$	$17N/12-6$	$17N/12$	$13N/5-9$	$13N/5$
$M(N)$	$N/6$	$N/6$	$N/5-1$	$N/5$

Table 3. Graphitic lattice ZZ_5: topological descriptors for the 24 vertices V of the unit cell embedded in the lattice fragment made by $\ell = 7$ cells; we have for this graphitic portion $N = 168$, $W = 151{,}200$; $M = 28$, $L = 232$.

V	$\{b_{im}\}$	$w_i/2$	Unit cell view
$^{*}V_{13}$	3 6 9 12 15 17 17 16 15 14 13 12 12 6	$^{*}658$	
$^{*}V_{12}$	3 6 9 12 15 17 17 16 15 14 13 12 11 6 1	$^{*}659$	
$^{*}V_{14}$	3 6 9 12 15 17 17 16 15 14 13 12 7 6 5	$^{*}663$	
$^{*}V_{11}$	3 6 9 12 15 17 17 16 15 14 13 11 6 6 6 1	$^{*}666$	
$^{*}V_{9}$	3 6 9 12 14 15 16 16 15 14 14 14 13 6	$^{*}670$	
$^{*}V_{8}$	3 6 9 12 14 15 16 16 15 14 14 14 12 6 1	$^{*}671$	
V_{18}	3 6 9 12 14 15 16 16 15 14 14 14 8 6 5	675	
V_{15}	3 6 9 12 14 15 16 16 15 14 14 13 7 6 6 1	678	
V_{17}	3 6 9 11 12 13 14 15 16 16 15 14 14 8 1	694	
V_{16}	3 6 9 11 12 13 14 15 16 16 15 14 13 8 2	695	
V_{10}	3 6 9 11 12 13 14 15 16 16 15 14 9 8 6	699	
V_{7}	3 6 9 11 12 13 14 15 16 16 15 14 9 7 6 1	700	
V_{5}	3 6 8 9 10 11 13 15 16 16 16 16 15 9 3 1	728	
V_{4}	3 6 8 9 10 11 13 15 16 16 16 16 15 9 2 1 1	729	
V_{22}	3 6 8 9 10 11 13 15 16 16 16 16 11 9 7 1	732	
V_{19}	3 6 8 9 10 11 13 15 16 16 16 15 10 9 8 2	735	
V_{21}	3 5 6 7 9 11 12 13 15 17 17 16 16 11 5 3 1	772	
V_{20}	3 5 6 7 9 11 12 13 15 17 17 16 15 11 6 3 1	773	
V_{6}	3 5 6 7 9 11 12 13 15 17 17 16 12 11 9 3 1	776	
V_{3}	3 5 6 7 9 11 12 13 15 17 17 16 12 11 9 2 1 1	777	
V_{1}	2 3 5 7 8 9 11 13 14 15 17 18 17 12 7 5 3 1	824	
V_{2}	2 3 5 7 8 9 11 13 14 15 17 18 17 12 7 5 2 1 1	825	
V_{23}	2 3 5 7 8 9 11 13 14 15 17 18 14 12 10 5 3 1	827	
V_{24}	2 3 5 7 8 9 11 13 14 15 17 15 13 11 10 8 3 2 1	838	

Notes: Vertex V_{13} is the minimal vertex of this graph. The six starred sites are confirmed to be the most compact vertices in the graph; therefore, the shaded central ring $\mathcal{H}$ is also very stable.

topological potential W generates barriers to topological variation of stable sites in order to keep low its global value.

The central hexagon $\mathcal{H}$ of Figure 4 is the minimal vertex of the dual lattice of ZZ_5^D (Figure 5). Any ring of the direct graph ZZ_5 generates a vertex in the dual graph with a number of bonds equal to the number of its edges. Therefore, a part from peripheral rings, any hexagons of ZZ_5 will correspond to a six-connected node of the dual graph (see Figure 5). Table 2 gives polynomials of $W(N)$, $L(N)$, $M(N)$ also for the dual lattice ZZ_5^D, whereas the formulas for the minimal dual vertex A_1 of ZZ_5^D are (see Figure 5)

$$\underline{w} = w_1 = \frac{N^2}{20} + 20, \quad \text{for the dual graph } ZZ_5^D, \tag{3.3a}$$

$$\underline{w} = w_1 \rightarrow \frac{N^2}{20}, \quad \text{when N} \rightarrow \infty, \quad \text{for the dual graph } ZZ_5^D. \tag{3.3b}$$

Quantity w_1 is divided by 2 in Equation (2.2) that produces $W(N)$ polynomials (Table 2). We note again that, in the dual lattice of Figure 5, the minimal vertex A_1 corresponds to the central hexagon $\mathcal{H}$ of the direct graph in Figure 4. Moreover, in ZZ_5^D, a new topological symmetry arises between A_1 and A_6 that share the same WW, thus $w_6 = w_1$. Our computations show (Tables 2 and 4) that in ZZ_5^D polynomial laws for $W(N)$, $M(N)$, w_1 stabilise for $\ell \geq 5$ ($N \geq 50$); again, only odd ℓ values are used in this paper.

We introduce the *topological efficiency index* ρ_G, a new topological invariant that measures graph efficiency in compactly filling the space when compared to its minimal vertex,

$$\rho_G = \frac{2W}{N\underline{w}}, \quad \text{with } \rho_G \geq 1. \tag{3.4}$$

From Equation (2.3b), we understand how ρ_G works: the minimal vertex is compactly embedded in the graph and gives the lowest contribution to $W(N)$, therefore being the best-performing sites in the overall graph in terms of compactness. Thus, if all sites would perform in a similar way, the resulting graph would be a successful and compact topological structure with a $W(N)$ value

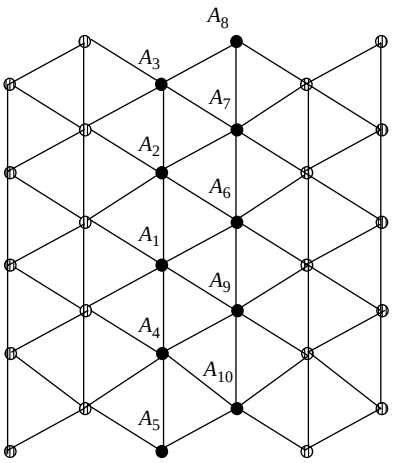

Figure 5. Graphitic dual lattice ZZ_5^D with $\ell = 3$ size; its unit cell includes 10 six-connected bulleted nodes corresponding to the hexagons 1–10 depicted in Figure 4(a). Vertex A_1 corresponds to the shaded central hexagon $\mathcal{H}$ in Figure 4.

close to $N/2$ times $\underline{w}$ as per previous Equation (2.3b). Topologically efficient graphs will then grow in the space by keeping their ρ_G values close to 1. This index provides valid topological information for direct and dual graphs. For infinite connected graphs, the optimal condition $\rho_G = 1$ may be true only for closed lattices. Now, we have enough control on topological descriptors to make some considerations about the ZZ_5^D graphitic fragment. From the dual Wiener-index asymptotic value (Table 2) and the WW value for the minimal vertex A_1 (Equations (3.3b)), we compute the efficiency index ρ_G of the graph $G = ZZ_5^D$ in the limit of large N by a simple application of Equation (3.4),

$$\rho_G = \frac{4}{3} = 1333, \quad \text{when } N \to \infty, \quad \text{for the dual graph } ZZ_5^D. \tag{3.5}$$

When we compute the corresponding asymptotic values (from Equation (3.1) and Table 2) for the direct graph ZZ_5, we obtain the same ratio $\rho_G = 4/3$ that appears to be a sort of *universal topological signature* of this structure valid for both representing graphs, the direct ZZ_5 and the dual ZZ_5^D one,

$$\rho_G = \frac{4}{3} = 1333, \quad \text{when } N \to \infty, \tag{3.6}$$

for the direct graph ZZ_5 also. This intriguing *symmetry* of ρ_G will be the subject of further investigations; it also indicates that our choice to work in the dual space constitutes a proper computational approach that does not limit the significance of the main results reported in this paper.

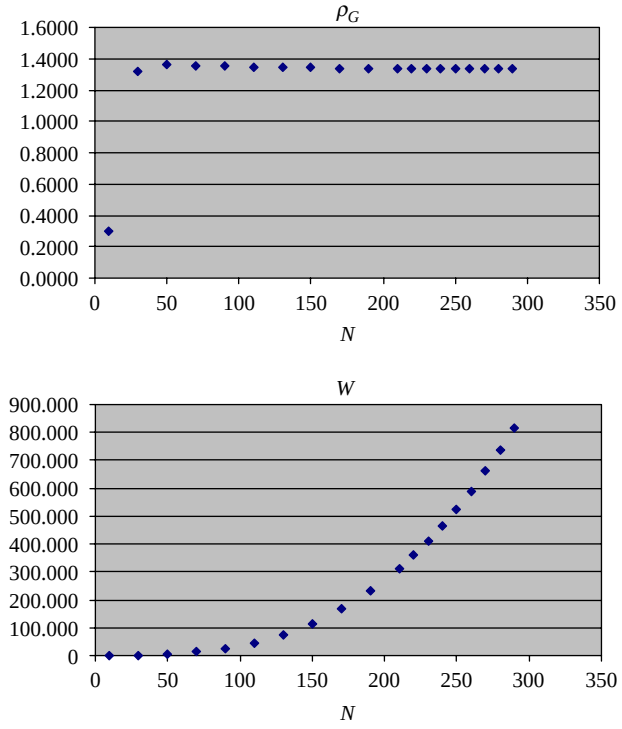

Figure 6. Top: Behaviour of the graph descriptor ρ_G for the graphitic dual lattice ZZ_5^D at increasing N (with $N = 10\ell$); the 4/3 limit of Equation (3.5) is quickly reached. Bottom: Wiener-index $W(N)$ cubic growth for the ZZ_5^D graph (Table 2).

When the index ρ_G remains close to its lower limit 1, the graph G shows higher topological compactness if compared to other graphs made of similar building units; in the case of the graphenic structures under study in this work, the building units are hexagonal rings (in the direct space) or six-connected vertices (in the dual space). According to our model, chemical structures with a relatively high topological compactness will have certain chemical stability and probability of formation. The rational value given in Equation (3.5) measures the topological efficiency of the ZZ_5^D fragment of graphite in filling the dual space when its size becomes infinite in one dimension. The curve in Figure 6 represents ρ_G values for ZZ_5^D for low values of N. Our computations show the tendency of this index to approach its theoretical limit 4/3 for relatively small values of N when the lattice still has a low number of cells.

Previous results characterise the infinite monodimensional graphitic fragment, and we use them to compare similar topological features of alternative graphenic structures; moreover, the fact that graphite fragments are surely formed in conditions of high temperature will allow us to make chemical considerations on those alternative structures.

4. Topological analysis of a graphenic fullerene-like lattice

We now apply our topological model to the (infinite) fullerene-like graph F (Figure 7) formed by adding concentric hexagonal rings around the central pentagon. In the literature, these structures are often called *nanocones*. To keep our computations simple, we prefer to work in the dual space; then we indicate with F^{D} the dual graph of this fullerene portion with a single pentagon (one five-connected vertex V_1) surrounded by circles of hexagons (six-connected vertices); the first circle contains the five hexagons 2, 3, 4, 5, 6 (see Figure 7). When we add $N-1$ hexagons, this fullerenic dual lattice exhibits peculiar topological descriptors. The graphenic infinite lattice has a natural topological generator given by the number f of circles of hexagons around the pivotal pentagon as shown in Figure 7; the total number N of graph faces (we remember that $N-1$ faces are hexagonal) may be written as a second-degree polynomial of the lattice generator f,

$$N = 1 + \frac{5(f^2 + f)}{2}, \quad f \geq 0. \tag{4.1}$$

In Equation (4.1), the value $f = 0$ corresponds to a graph with a sole pentagon. Table 4 lists the original polynomial laws for the topological descriptors of F^{D}. Table 5 reports the first example of the Wiener index (and other topological descriptors) with a polynomial dependence of f instead of N; to our knowledge, this is the first documented generalisation of Bonchev and Mekenyan discovery made in [19].

We report more topological results on F^{D}. For $f = 1$, $N = 6$, we have $W = 20$, $M = 2$, $L = 10$. The shaded central pentagon in Figure 7 is the graph minimal vertex A_1 having $\underline{w} = 5$ and WS string with only first-neighbours contacts $\{b_{1m}\} = \{5\}$; the remaining graph sites A_i for $i = 2, \ldots, 6$ (they are the five hexagons surrounding A_1) have common topological descriptors WW ($w_i = 7$) and WS ($\{b_{im}\} = \{3\ 2\}$). Table 6 reports the case $f = 2$, $N = 16$; we have $W = 255$, $M = 4$, $L = 35$. Vertex A_1 still remains the minimal vertex of this graphenic structure with two circles of hexagons. The five inner hexagons are obviously equivalent sites with equal WS strings $\{b_{im}\} = \{6\ 6\ 3\}$ for $i = 2$–6. From Equation (2.11), we derive topological dimensionality from the leading power $\underline{k}$ of the function, giving $W(N)$ in the asymptotic limit for graphitic and fullerenic graphs. From Tables 2 and 5, we derive the following limits:

$$W(N) \rightarrow N^{5/2}, \quad \text{for the dual graph } F^{\mathrm{D}}, \tag{4.2}$$

$$W(N) \rightarrow N^{3}, \quad \text{for the dual graph } \mathrm{ZZ}_5^{\mathrm{D}}. \tag{4.3}$$

Equations (4.3) and (2.11) imply $d_{\mathrm{T}} = 1$ for the graphitic lattice $\mathrm{ZZ}_5^{\mathrm{D}}$, whereas from Equation (4.2) we originally derive the topological dimensionality $d_{\mathrm{T}} = 2$ for fullerenic infinite lattices. Fullerene portions show a topological growth of W lower than $\mathrm{ZZ}_5^{\mathrm{D}}$ or any other polymer. It is quite noticeable to see how $\mathrm{ZZ}_5^{\mathrm{D}}$ and F^{D} have huge topological differences and also if they are made of the same building units (six-connected nodes).

Resuming,

$$d_{\mathrm{T}} = 2, \quad \underline{k} = \frac{5}{2} \quad \text{for the dual graph } F^{\mathrm{D}}, \tag{4.4a}$$

with $\underline{k}$ a value lower than

$$d_{\mathrm{T}} = 1, \quad \underline{k} = 3 \quad \text{for the dual graph } \mathrm{ZZ}_5^{\mathrm{D}}. \tag{4.4b}$$

An evident topological effect of the dimensionality of F^{D} is the immediate stabilisation of the polynomial formulas

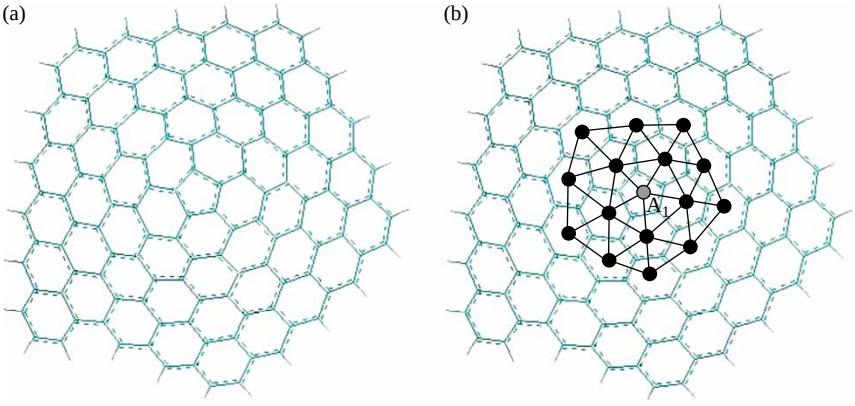

Figure 7. Fullerene-like graph F (a) in the direct space and (b) in the dual space F^{D} with dual vertices represented in black; with the sole exception of the shaded pentagon A_1 at the centre of this nanocone; for simplicity only the first two circles ($f = 2$, where the number of circles f is the lattice generator) of hexagonal faces around the central pentagon are represented.

Table 4. Lattice ZZ_5^D: topological descriptors for 10 vertices of the dual unit cell embedded in two different lattice fragments $\ell = 3$, $N = 30$, $W = 4937$, $M = 7$, $L = 69$ (Figure 5) and $\ell = 5$, $N = 50$, $W = 4937$, $M = 9$, $L = 121$.

ZZ_5^D, $\ell = 3$, $N = 30$, $W = 1288$			ZZ_5^D, $\ell = 5$, $N = 50$, $W = 4937$		
V	$\{b_{im}\}$	$w_i/2$	V	$\{b_{im}\}$	$w_i/2$
A_1	6 12 10 1	32	A_1	6 12 14 12 5	72.5
A_6	6 12 10 1	32	A_6	6 12 14 12 5	72.5
A_2	6 11 9 3	33.5	A_2	6 11 13 12 7	75
A_9	6 11 9 3	33.5	A_9	6 11 13 12 7	75
A_4	6 9 8 5 1	36.5	A_4	6 9 11 14 8 1	79.5
A_7	6 9 8 5 1	36.5	A_7	6 9 11 14 8 1	79.5
A_3	5 7 8 6 3	41	A_3	5 7 11 13 10 3	86
A_{10}	5 7 8 6 3	41	A_{10}	5 7 11 13 10 3	86
A_5	3 7 7 6 5 1	46.5	A_5	3 7 9 13 11 5 1	94
A_8	3 7 7 6 5 1	46.5	A_8	3 7 9 13 11 5 1	94

Notes: Nodes A_1 and A_6 show the minimum w_i values and are therefore the minimal vertices of this graph; vertex A_1 corresponds to the topologically most stable hexagon $\mathcal{H}$ of the direct lattice in Figure 4.

in Table 5 that are valid for $f \geq 1$ with $N(f)$ given by Equation (4.1). This is not true for ZZ_5^D, whose topological descriptors, given in Table 2, need specific ℓ thresholds before reaching valid polynomial interpolations.

- From a chemical point of view, the reduced $\underline{k}$ value expressed by Equation (4.4a) constitutes the first topological evidence in favour of the formation of fullerenic nanostructure; F^D graphs fill the space in a more efficient way with respect to the reference graphitic ZZ_5^D lattice with $d_T = 1$.

Both lattices are practically made of the same numbers of hexagons (six-connected vertices in the dual lattices), and the above result confers to the fullerenic lattice F^D a significant probability of formation when compared to the graphitic ZZ_5^D lattice. Thus, during inception and particle growth in high-temperature combustion conditions, the graphene sheets with a fullerene-like structure have the same topological possibility of forming the commonly known graphene sheets free from fullerene-like defects.

Figure 8 gives $W(N)$ curves for infinite graphs F^D and ZZ_5^D and points out that $W(N)$ grows faster for the graphitic fragments. Thus, for any values of N, the structure F^D presents a higher compactness (having a lower W value) when compared to the graphitic graph ZZ_5^D, and this is true not only in the infinite limit (see asymptotic Equations (4.2) and (4.3)) but also for low values of N when lattices are made of a few hundreds of hexagons (Figures 5 and 7(b)).

Table 5. Topological descriptors for the dual fullerenic lattice F^D (Figure 7): exact formulas for the Wiener index $W(f)$, the number of chemical bonds $L(f)$, the maximum graph distance $M(f)$ and their values in the infinite N limit are given in dual space; f is the nanocone lattice generator.

Descriptor	Dual space F^D	$N \to \infty$
$W(f)$	$(62f^5+155f^4+160f^3+85f^2+18f)/24$	$31/12f^5$
$L(f)$	$(15f^2+5f)/2$	$15/2f^2$
$M(f)$	$2f$	$2f$

Fullerene fragments show a higher topological compactness during their growth; this is an important signal about the non-negligible probability of finding fullerene-like structures on graphene sheets on carbon black or on amorphous carbon in general.

We derive now a complementary indication about the F^D graph growing efficiency. From Equation (3.4), we numerically derived the upper limit to its *topological efficiency index*,

$$\rho_G(F^D) \leq 1273, \quad N \to \infty, \quad \text{for the dual graph } G = F^D. \tag{4.5}$$

Comparing ρ_G values (3.5) and (4.5), we obtain the quantitative evaluation of the gap in topological efficiency between fullerenic F^D and graphitic ZZ_5^D lattices that is valid at any comparable sizes N of their respective lattices,

$$\rho_G(F^D) < \rho_G(ZZ_5^D), \quad N \to \infty, \quad \text{for dual graphs } F^D \text{ and } ZZ_5^D, \tag{4.6}$$

Figure 9 shows that also for low values of the number of hexagons, the graph F^D has, for $N \geq 16$, the best topologically growing strategy when compared to ZZ_5^D; in the infinite lattice limit, this property is confirmed by Equation (4.6).

Table 6. Lattice topological descriptors for the 16 vertices V of the F^D graph when $f = 2$, $N = 16$; summing the last column, one gets the Wiener index of the structure $W = 255$, $M = 4$, $L = 35$.

V	$\{b_{im}\}$	$w_i/2$
*A_1	5 10	*12.5
A_2	6 6 3	13.5
A_3	6 6 3	13.5
A_4	6 6 3	13.5
A_5	6 6 3	13.5
A_6	6 6 3	13.5
A_8	4 5 5 1	16.5
A_{10}	4 5 5 1	16.5
A_{12}	4 5 5 1	16.5
A_{14}	4 5 5 1	16.5
A_{16}	4 5 5 1	16.5
A_7	3 5 4 3	18.5
A_9	3 5 4 3	18.5
A_{11}	3 5 4 3	18.5
A_{13}	3 5 4 3	18.5
A_{15}	3 5 4 3	18.5

Note: Starred site A_1 remains the minimal vertex of this graph.

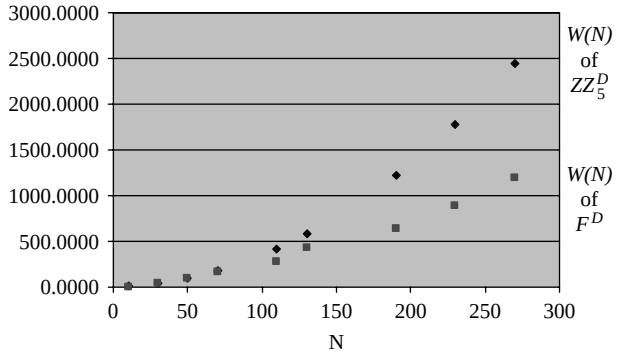

Figure 8. Wiener-index curves for the two graphenic structures in the dual space as a function of increasing N: top curve gives $W(N)$ for the dual lattice ZZ_5^D and the bottom one refers to the fullerenic dual graph F^D.

In conclusion, we largely exploited the usage $W(N)$ as the topological potential that, *when applied to similar systems*, tends to select the most compact one; this *topological minimum principle* has been applied to graphenic lattices (made by similar hexagonal subunits) pointing out that:

(i) during its growth, F^D presents a lower asymptotic growth in their Wiener index (Equations (4.4a) and (4.4b) and Figure 8) with respect to ZZ_5^D, and this fact makes this lattice relatively more compact and potentially more stable than the reference graphitic ZZ_5^D;
(ii) moreover, the topological lattice descriptor ρ_G, Equation (4.6), tells us that F^D fills the space in a very efficient way around its most stable site (we will see in the following paragraphs that this site migrates during lattice expansion); the graphitic lattice ZZ_5^D does not exhibit a similar topological ability (see Figure 9).

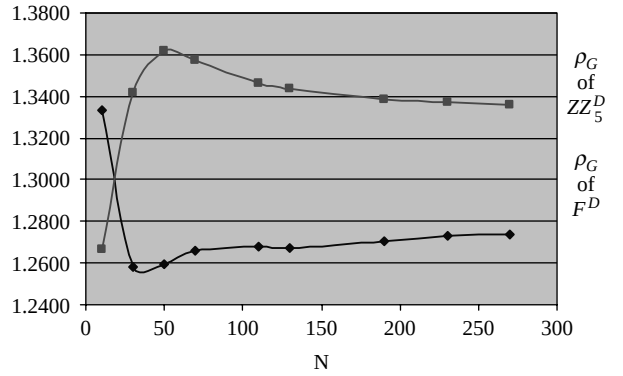

Figure 9. The two plots report the topological efficiency of F^D (bottom) and ZZ_5^D (top) when few hundreds of hexagonal rings are added to both lattices; the relationship $\rho_G(F^D) < \rho_G(ZZ_5^D)$ is valid for the growing steps with $N \geq 16$.

The above relevant theoretical findings have strong chemical implication during the process of formation of carbon black.

Lastly, we report here a further topological effect induced on F^D by a non-integer $\underline{k}$ value. We may in fact verify that, by increasing the values of N, its minimal vertices *migrate* along the graph following a quite organised path (Figure 10). This means that the fullerene fragment F^D does not have any vertex that, during its growth, remains topologically the most stable. On the contrary, the central hexagon $\mathcal{H}$ of the reference lattice ZZ_5^D (Figure 5, site A_1) maintains its role of the minimal vertex and, at any graph size ℓ, generates the lowest contribution to $W(N)$ expressed by Equation (3.2a) that stabilises for $\ell \geq 5$ ($N \geq 50$). From our computation on F^D, we discovered that the graph minimal vertex changes its position during lattice growth. Initially, the minimal vertex corresponds to the shaded central pentagon A_1 in Figure 7(b). Then, we enlarge the fullerenic fragment by adding new concentric circles of hexagonal faces and, when N reaches the thresholds $N \geq 51$, the minimal vertex jumps from A_1 to B and its four symmetric vertices (see Figure 10). By increasing N again, the minimal vertex becomes more and more distant from the central pentagon A_1 reaching node C (and its symmetric sites), then D, E and so on. Topologically, minimal vertices are the most stable ones according to their low WW (2.2). Table 7 gives numerical variations of $\underline{w}$ and $\rho_G(F^D)$, evidencing that when the lattice generator is equal to or greater than 4 $f \geq 4$ ($N \geq 51$), the pentagon A_1 (Figures 7(b) and 10)

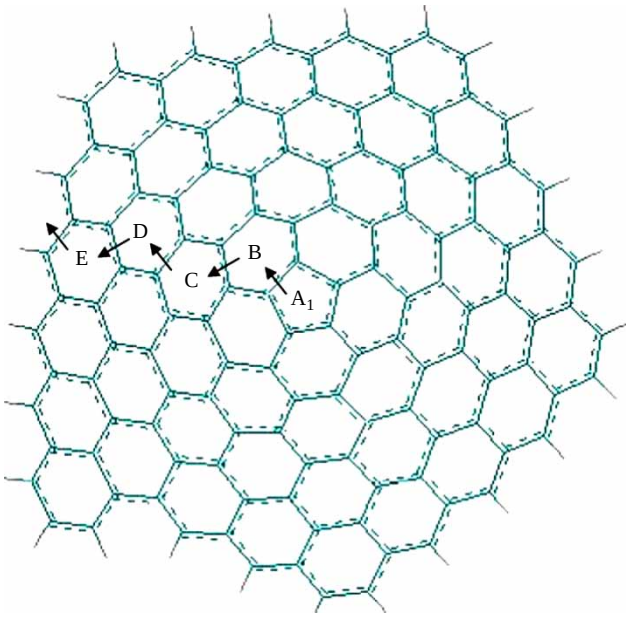

Figure 10. Migration of minimal vertices A_1, B, C, D, E at increasing values of N in the dual graph F^D (symmetric vertices are not shown); they correspond to stable faces on the fullerenic direct nanocone F.

Table 7. Lattice topological descriptors $\underline{w}$ and ρ_G for F^D as a function of N; the most stable site migrates during lattice growth.

f	N	V	$w_i/2$	ρ_G
1	6	A_1	2.5	1.333
4	51	B	74.5	1.259
8	181	C	499	1.270
16	681	D	3649	1.272
19	951	E	6023	1.272
27	1891	F	16,890	1.272
31	2481	G	25,381	1.272

Note: Minimal vertex starts on A_1, the central pentagon, and passes on B then on C, $D, E, \ldots$ in an unending migration process along the zigzag path shown in Figure 10. Last column gives ρ_G values whose curve is represented in Figure 9 (bottom line).

loses its role of the most stable node in favour of one of the hexagon in the graph. The splitting $(w_1 - \underline{w})$ between WW contributions of A_1 and the minimal vertex presents typical oscillations documented here for the first time in Figure 11. Peaks in this curve correspond to a region where the $(w_1 - \underline{w})$ gap reaches a local maximum enhancing the probability of having A_1 modifications. Our model shows that the central pentagon A_1 in the fullerene remains the stable vertex until the fourth circle of hexagons is added to the structure (Table 7 and Figure 10). After the threshold $f \geq 4$ ($N \geq 51$) site A_1 becomes less and less stable, the ratio $(w_1 - \underline{w})/\underline{w}$ augments until a shoulder in the region $7 \leq f \leq 10$ (Figure 11) when the Wiener potential weakly opposes topological variations of A_1. This pure topological mechanism practically turns pentagon reactivity on. This effect is enhanced at given graph sizes: for example, at $f = 11$, the fullerenic fragment is made of 330 hexagons and the ratio $(w_1 - \underline{w})/\underline{w}$ shows, in Figure 11, a local peak favouring the stability of vertex C of about 2.6% (see Table 7 and Figure 10). In conclusion, for any local peaks in Figure 11, one may expect a relatively higher reactivity of pentagon A_1 of the fullerene-like nanostructures represented in Figure 7(b).

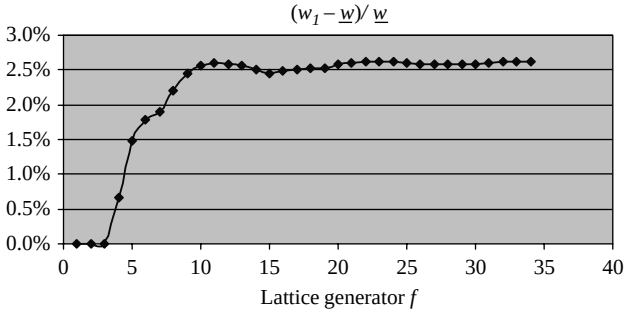

Figure 11. Typical oscillations of the $(w_1 - \underline{w})/\underline{w}$ ratio; the barrier effect of the Wiener potential $W(N)$ against topological variations of the pentagonal site diminishes in correspondence with local peaks of the curve.

It is worthwhile to notice the *double role* played by the central pentagon A_1 in fullerene F^D graph evolution: on the one hand, its presence favours the growth of a curved, fullerene-like lattice with a low $W(N)$, high compactness and high topological efficiency; on the other hand, after a certain lattice size, this pentagonal face abandons its role of topologically most stable site of the graph and presents a certain chemical reactivity. Resuming:

(iii) pentagonal vertex A_1 in Figures 7 and 10 acts as the topological seed of the fullerenic nanocone graph F^D and allows the growth of this structure that successfully competes with fragments of the graphitic hexagonal lattice; the same A_1 pentagon, when the size of the fullerene fragments is big enough, loses it stability and presents a topological tendency to become the reactive region in F^D.

These results are really relevant because they are in line with the well-known chemical reactivity of fullerenes and, consequently, of the fullerene-like structures inserted in graphene sheets. In fullerenes, the reactivity is concentrated in the proximity of the pentagonal sites and all the additions occur at the radialene bonds from the edge of pentagonal sites. This implies that fullerene chemistry can be extended to carbon surfaces possessing fullerene-like structures.

5. Conclusions

Introduction of the new conjecture on Wiener-index behaviour $W(N^{\underline{k}})$ for infinite chemical graphs with topological dimensionality $d_T > 1$ represents the main theoretical general contribution of this paper. Detailed topological computations applied to fullerene-like infinite structures compared to graphitic infinite fragments document here that topological compactness and topological efficiency ρ_G (a newly introduced lattice descriptor) are powerful theoretical tools to discriminate between these classes of complex chemical structures. The usage of the Wiener index as pure topological potential energy of graphenic infinite structures produces, in fact, interesting results, assigning to fullerene-like nanostructures a non-negligible probability of formation on graphene sheets on carbon black or on amorphous carbon in general. Moreover, our topological model shows that the central pentagonal ring becomes chemically reactive when the fullerene fragment reaches certain sizes.

Acknowledgements

We wish to thank Prof. Gianni Strazzulla for his helpful discussion. We wish to acknowledge ASI, the Italian Space Agency, for the partial support of the present work under the Contract No. I/015/07/0 (Studi di Esporazione del Sistema Solare).

References

[1] F. Cataldo, *Role of fullerene-like structures in carbon black and their interaction with dienic Rubber*, Fullerene Sci. Technol. 8 (2000), pp. 105–112.

[2] F. Cataldo, *The impact of fullerene-like concept in carbon black science*, Carbon 40 (2002), pp. 157–162.

[3] M. Pontier-Johnson, R.W. Locke, J.B. Donnet, T.K. Wang, C.C. Wang, and P. Bertrand, *Carbon black and fullerenes: New discoveries in early formation mechanisms and nucleation*, Rubber Chem. Technol. 73 (2000), pp. 875–888.

[4] W.J. Grieco, J.B. Howard, L.C. Rainey, and J.B. Van der Sande, *Fullerenic carbon in combustion-generated soot*, Carbon 38 (2000), pp. 597–614.

[5] K.H. Homan, *Fullerenes and soot formation. New pathways to large particles in flame*, Angew. Chem. Int. Ed. 37 (1998), pp. 2434–2451.

[6] J.Y. Huang, H. Yasuda, and H. Mori, *Highly curved carbon nanostructures produced by ball milling*, Chem. Phys. Lett. 303 (1999), pp. 130–134.

[7] R.E. Nightingale, *Nuclear Graphite*, Academic Press, New York, 1962.

[8] F. Cataldo, *Raman spectra on radiation-damaged graphite*, Carbon 38 (2000), pp. 634–636.

[9] F. Cataldo, *Fullerene-like structures as interaction sites between rubber and carbon black*, Macromol. Symp. 228 (2005), pp. 91–98.

[10] F. Cataldo and M. Pontier-Johnson, *Recent discoveries in carbon black formation and morphology and their implications on the structure of the interstellar carbon dust*, Fullerenes Nanot. Carbon Nanostruct. 10 (2002), pp. 1–14.

[11] F. Cataldo, *The possible role of fullerene-like structures present on the surface of the interstellar carbon dust in the formation of H_2 in space*, Fullerenes Nanot. Carbon Nanostruct. 11 (2003), pp. 317–331.

[12] F. Cataldo, *Fullerane, the hydrogenated C_{60} fullerene: Properties and astrochemical considerations*, Fullerenes Nanot. Carbon Nanostruct. 11 (2003), pp. 295–316.

[13] H. Wiener, *Structure determination of paraffin boiling points*, J. Am. Chem. Soc. 69 (1947), pp. 17–20.

[14] H. Hosoya, *Topological index. A newly proposed quantity characterizing the topological nature of structural isomers of saturated hydrocarbons*, Bull. Chem. Soc. Jpn 44 (1971), pp. 2332–2339.

[15] E. Estrada, O. Ivanciuc, I. Gutman, A. Gutierrez, and L. Rodriguez, *Extended Wiener indices. A new set of descriptors for quantitative structure–property studies*, New J. Chem. 20 (1998), pp. 819–822.

[16] W.G. Yan and Y.N. Yeh, *Connections between Wiener index and matchings*, J. Math. Chem. 39 (2) (2006), pp. 389–399.

[17] E.A. Castro, I. Gutman, D. Marino, and P. Peruzzoa, *Upgrading the Wiener index*, J. Serb. Chem. Soc. 67 (10) (2002), pp. 647–651.

[18] R. Todeschini and V. Consonni, *Handbook of Molecular Descriptors*, Wiley-VCH, Weinheim, 2000.

[19] D. Bonchev and O. Mekenyan, *A topological approach to the calculation of the Π-electron energy and energy gap of infinite conjugated polymers*, Z. Naturforsch. 35a (1980), pp. 739–747.

[20] O. Ori and M. D'Mello, *A topological study of the structure of the C_{76} fullerene*, Chem. Phys. Lett. 197 (1–2) (1992), pp. 49–54.

[21] O. Ori and M. D'Mello, *Analysis of the structure of the C_{78} fullerene: A topological approach*, Appl. Phys. A Solids Surfaces 56 (1) (1993), pp. 35–39.

[22] K. Balasubramanian, *Distance spectra and distance polynomials of fullerenes*, J. Phys. Chem. 99 (1995), pp. 10785–10796.

[23] A.A. Dobrynin, I. Gutman, S. Klavžar, and P. Žigert, *Wiener index of hexagonal systems*, Acta Appl. Math. 72 (3) (2002), pp. 247–294.

[24] P. Fowler, *Resistance distances in fullerene graphs*, Croat. Chem. Acta 75 (2) (2002), pp. 401–408.

[25] Z. Slanina, M.C. Chao, S.L. Lee, and I. Gutman, *On applicability of the Wiener index to estimate relative stabilities of the higher-fullerene IPR isomers*, J. Serb. Chem. Soc. 62 (1997), pp. 211–217.

[26] O. Ori and P. Marenzoni, *Parallel computation of the matrix of the chemical distances on the connection machine*, Mol. Sim. 11 (1993), pp. 365–372.